Comparison of DC High-Frequency Performance of Zinc-Doped and Carbon-Doped InP/InGaAs HBTs Grown by Metalorganic Chemical Vapor Deposition

Delong Cui, Dimitris Pavlidis, *Fellow, IEEE,* Shawn S. H. Hsu, and Andreas Eisenbach

***Abstract*—Zinc and carbon-doped InP/InGaAs heterojunction bipolar transistors (HBTs) with the same design were grown by metalorganic chemical vapor deposition (MOCVD). Dc current gain values of 36 and 16 were measured for zinc and carbon-doped HBTs, respectively, and carrier lifetimes were measured by time-resolved photoluminescnce to explain the difference. Transmission line model (TLM) analysis of carbon-doped base layers showed excellent sheet-resistance (828 $\Omega/\square$ for 600 Å base), indicating successful growth of highly carbon-doped base (2×10^{19} cm^{-3}). The reasons for larger contact resistance of carbon than zinc-doped base despite its low sheet resistance were analyzed. f_T and $f_{\max}$ of 72 and 109 GHz were measured for zinc-doped HBTs, while 70-GHz f_T and 102 GHz $f_{\max}$ were measured for carbon-doped devices. While the best performance was similar for the two HBTs, the associated biasing current densities were much different between zinc (4.0×10^4 A/cm^2) and carbon-doped HBTs (2.0×10^5 A/cm^2). The bias-dependant high-frequency performance of the HBTs was measured and analyzed to explain the discrepancy.**

I. Introduction

InP-based heterojunction bipolar transistors (HBTs) have demonstrated excellent high-frequency performance [1]–[5] and have been employed in high-speed IC applications [6], [7]. Traditionally, Zn and Be are used as base dopants for InP/InGaAs HBTs. However, the relatively high diffusivity of zinc dopants could cause severe problems in terms of device processing and reliability [8]–[10]. On the other hand, carbon is a very attractive substitute as a p-type dopant for InGaAs material due to its remarkably low diffusion coefficient. Heavily carbon doped p-type layers have been successfully grown by MOCVD [11], [12], metalorganic molecular beam epitaxy (MOMBE) [13]–[16], as well as chemical beam epitaxy (CBE) [17], [18]. However, the amphoteric nature of carbon dopant makes it necessary to employ low growth temperature and low V/III ratio in MOCVD growth to realize p-type doping for InGaAs material. This could lead to the degradation of material quality of InGaAs:C layers [19]. Large amount of hydrogen passivation of carbon dopants also makes it more difficult using MOCVD to grow heavily p-type carbon-doped InGaAs layers than MBE. Use of N_2 as carrier gas was proposed to lessen this problem [20]. Moreover, the growth interruption introduced by the low temperature growth of the carbon-doped base in an HBT structure could lead to the degradation of base-emitter and base-collector junction and hence degrade even further the electrical performance of carbon-doped HBTs.

Recently, carbon-doped InP/InGaAs HBTs have been grown by MOCVD. 62-GHz f_T and 42 GHz $f_{\max}$ have been achieved by using TEGa and CCl_4 as precursors [21], [22]. A two-step MOCVD growth procedure has been also proposed to increase the $f_{\max}$ of carbon-doped HBTs to 160 GHz [23]. However, it requires regrowth and the regrowth temperature must also be low to prevent rehydrogenation during deposition. Moreover, the optimum biasing current density J_C for best f_T and $f_{\max}$ was found to be 2.3×10^5 A/cm^2 and 1.6×10^5 A/cm^2, which is considerably higher than that of normal zinc-doped or Be-doped HBTs, which is in the middle range of 10^4 A/cm^2. It is therefore of great interest not only to study the high-frequency issues of carbon-doped HBTs but also to compare their difference with zinc-doped devices.

This paper reports the first systematic comparative study of zinc and carbon-doped HBTs. Successful growth and fabrication of carbon-doped InP/InGaAs HBTs is reported by MOCVD. A HBT structure was also grown and fabricated using the same procedure, which employed zinc rather than carbon as base dopant. The dc and high frequency performance of these HBTs was measured and f_T and $f_{\max}(U)$ of 72 GHz and 109 GHz were achieved for zinc-doped HBTs while f_T and $f_{\max}(U)$ of 70 GHz and 102 GHz were demonstrated for carbon-doped HBTs. Although the optimum microwave performance was similar, these two types of HBTs show considerable difference in terms of not only dc gains but also optimum biasing conditions for microwave performance. Time resolved photoluminescence characterization was performed for heavily doped p-type InGaAs:C and InGaAs:Zn layers to explain the dc gain difference. The microwave performance of zinc and carbon-doped HBTs under various biasing conditions was also measured and a simple method was employed to analyze and compare the performances of these two types of HBTs and to explain the observed discrepancy in terms of biasing required for best performance.

II. Material Growth and Device Fabrication

The HBT layers were grown using an in-house EMCORE GS3200 low pressure metalorganic chemical vapor deposition system (LP- MOCVD), which employs a stainless steel reactor in vertical transport configuration. The carrier gas is H_2 and purified by Pd-cell diffusion. Hydrides and alkyls are carried in two seperate lines to the growth reactor. The substrate is rotated

Manuscript received September 4, 2001; revised February 19, 2002. This work was supported by ARO MURI DAAH04-96-1-0001. The review of this paper was arranged by Editor M. Anwar.

The authors are with the Department of Electrical Engineering and Computer Science, The University of Michigan, Ann Arbor, MI 48104 USA (e-mail: pavlidis@umich.edu).

Publisher Item Identifier S 0018-9383(02)04328-9.

0018-9383/02$17.00 © 2002 IEEE

at an optimized speed to compensate for the asymmetry of the reactor and a rotation speed of 100 rpm proved to produce the best uniformity across the wafer.

The group III metalorganics used in this study are all-methyl organometalic precursors: trimethylindium (TMIn) and trimethylgallium (TMGa). The group III precursors are stored in bubblers and are carried out to the growth reactor by H_2 carrier gas. Pure 100% AsH_3 and PH_3 are used for group V precursors. The system offers a double dilution system for two hydrides in order to provide a high dynamic range. Si_2H_6 (1% diluted in hydrogen) was employed as n-type dopant. Liquid diethylzinc (DEZn) and liquid carbon tetrabromide (CBr_4) were used for p-type doping purposes.

Except for highly carbon-doped p-type InGaAs layers, all the growth experiments were carried out at a growth temperature of 570 °C and V/III ratio of $\sim$ 20, which was optimized for the MOCVD growth system and proved to give good quality and reproducible epitaxy layers. For highly carbon-doped p-type layers, low growth temperature and low V/III ratio ($\sim$ 2) were employed in order to maximize the p-type doping concentration. A growth temperature of 450 °C was utilized in this study to achieve the best tradeoff between p-type doping concentration and good surface morphology.

A standard NPN InP/InGaAs HBT layer structure used in this study is shown in Table I. The profile includes a base thickness of 600 Å, a subcollector of 5000 Å uniformly doped to 2×10^{19} cm^{-3} and a collector of 5000 Å lightly doped to 5×10^{16} cm^{-3}. It uses 1500 Å and 700 Å InP as wide-band emitter layer with doping concentration of 5×10^{17} cm^{-3} and 2×10^{19} cm^{-3}, respectively. Finally a heavily doped InGaAs layer was deposited to improve the conductivity of the ohmic contacts. For both zinc and carbon-doped HBTs, the base-doping concentration was targeted to be 2×10^{19} cm^{-3}.

The zinc and carbon-doped InP/InGaAs HBT layers studied here were all of the same design as discussed earlier. The difference was in their base growth procedure and base dopants. For zinc-doped HBTs, all the layers were grown at a temperature of 570 °C. However, low growth temperature and low V/III ratio had to be used in order to realize p-type doping using carbon as dopant. Due to the difficulty in growth under low temperature and low V/III ratio, it was difficult to control both the compositional and doping concentrations. A growth temperature of 450 °C has been utilized in this study to minimize the degradation of epilayer morphology and maximize the p-type doping concentration at the same time. All other layers of carbon-doped HBTs were grown at 570 °C. The growth was therefore interrupted for approximately 3 min before the base growth to decrease the temperature from the optimized value (570 °C) to the low temperature (450 °C) required for carbon-doped base growth. After base growth, the growth was interrupted again and the system temperature was increased to the optimum value (570 °C) for emitter and emitter cap growth.

An all wet-etch based process developed at the University of Michigan, Ann Arbor, was employed in the fabrication to create trenches and isolation mesas. The base contacts were self-aligned to the emitters to reduce the base parasitic resistance. The emitters were protected and the wafers were then etched to the subcollector layer using the base contact as etch mask after base metallization. The resulting collector undercut led in reduction of the base-collector capacitance and thus enhanced $f_{\max}$ performance. The emitter and collector metal (n-metal) employed in this study was Ti/Pt/Au. The base metal (p-metal) employed in this study was Pt/Ti/Pt/Au.

TABLE I
STRUCTURE OF INP/INGAAS HBTS GROWN BY MOCVD

Layer	Type	Thickness (Å)
Emitter Cap	n^+-InGaAs	2000
	n^+-InP	700
Emitter	n-InP	1500
Spacer	i-InGaAs	100
Base	p^+-InGaAs	600
Collector	n^--InGaAs	5000
Subcollector	n^+-InGaAs	5000
Substrate	Semi-Insulating InP (001)	

Both zinc and carbon-doped InP/InGaAs HBTs were fabricated together using exactly the same processing steps. They shared the same wet etching solutions and their ohmic contacts were evaporated simultaneously on both wafers. Rapid thermal annealing (RTA) at 375 °C was carried out after base formation for 7 s in order to sinter the base contact. The variation in zinc and carbon-doped HBT characteristics due to processing could in this way be minimized so that their comparison could be meaningful. The observed differences, if any, are consequently expected to arise due to the nature of the base dopants, low growth temperature and low V/III ratio, which are necessary to improve the carbon incorporation efficiency in case of the carbon-doped InGaAs base. Another factor could be the interruption time introduced before and after carbon-doped base growth to adjust the growth temperature (450 °C) to the optimum growth temperature (570 °C) for collector, emitter and emitter cap growth; zinc-doped HBT layer growth was carried out at 570 °C for all the layers without any interruption time except for gas switching.

III. DC PERFORMANCE OF ZINC AND CARBON-DOPED INP/INGAAS HBTS

The common emitter current–voltage (I–V) characteristics of typical zinc and carbon-doped HBTs with emitter geometry of 1×10 μm^2 are shown in Fig. 1(a) and 1(b), respectively. As can be observed from the dc characteristics, carbon-doped HBTs show a dc gain of 16 while zinc-doped HBTs show a dc gain of 36, almost two times higher than carbon-doped HBTs. The offset voltage was found to be 0.2 V for both HBTs since it is determined by the difference in the turn-on voltages of the base-emitter and base-collector junctions and no obvious difference is evident in the junctions formed by zinc or carbon-doped InGaAs.

In order to explain the considerable difference in terms of dc gains for these two otherwise same HBT structures except for base dopants and base growth, heavily zinc and carbon-doped p-type InGaAs layers were characterized by time-resolved photoluminescnce and their carrier lifetime was evaluated. The InGaAs:C layers characterized had a doping concentration of 2×10^{19} cm^{-3} and the InGaAs:Zn layers had a doping concentration of 2.3×10^{19} cm^{-3}, as measured by Hall. The InGaAs:Zn showed a carrier lifetime of 53 ps, while InGaAs:C showed a carrier lifetime of 29 ps. The gain scales slightly different than predicted purely on the basis of carrier

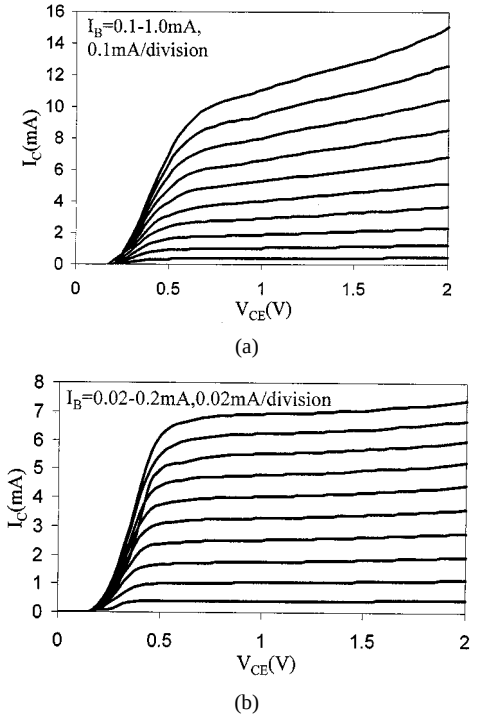

Fig. 1. (a) DC characteristics of $1 \times 10\ \mu m^2$ carbon-doped InP/InGaAs HBT and (b) DC characteristics of $1 \times 10\ \mu m^2$ zinc-doped InP/InGaAs HBT.

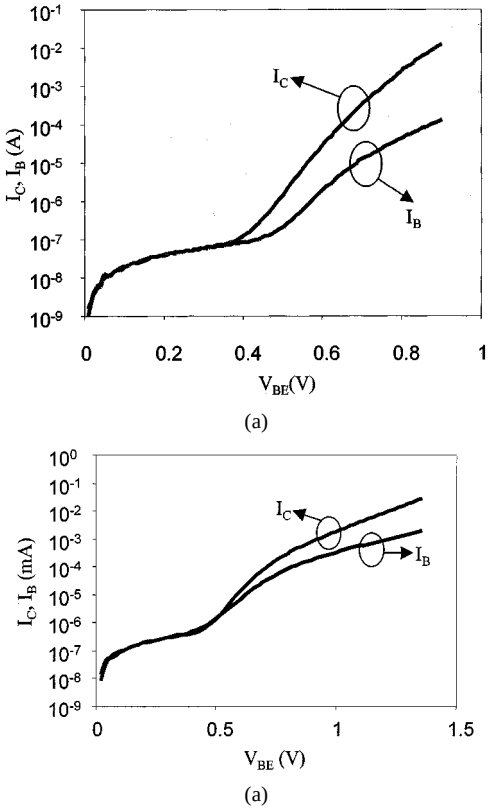

Fig. 2. (a) Gummel plot of $1 \times 10\ \mu m^2$ zinc-doped InP/InGaAs HBT and (b) Gummel plot of $1 \times 10\ \mu m^2$ carbon-doped InP/InGaAs HBT.

lifetime measurements (2.25 for dc gain and 1.82 for carrier lifetime measurement) due to the slight difference in doping concentration of the measured sample (a bulk layer was used for carrier lifetime measurement) and the actual base doping concentration in the device structure.

The previous measurements clearly show that InGaAs:C is relatively worse in terms of material quality than InGaAs:Zn if minority carrier lifetime is used as base of comparison. The degraded minority carrier lifetime performance of heavily doped p-type InGaAs:C directly leads to a considerably lower dc gain for carbon-doped HBTs. This is however, as expected due to the lower growth temperature and lower V/III ratio required to realize heavily p-type doped InGaAs:C layers. Both conditions, low growth temperature and low V/III ratio, would lead in material quality and surface morphology degradation, which can then turn into degradation of carrier lifetime.

The Gummel plot of the zinc-doped InP/InGaAs HBT is shown in Fig. 2(a). The extracted ideality factors for base and collector current are $n_B = 1.7$ and $n_C = 1.3$. The results agree with published results for InP/InGaAs HBTs [23]–[26], where n_C ranged from 1.02 to 1.5 and n_B ranged from 1.02 to 2.0. The Gummel plot of the carbon-doped InP/InGaAs HBT is shown in Fig. 2(b). The ideality factor for base current and collector current n_B and n_C are 2.2 and 1.6, respectively. Both ideality factors are considerably larger compared with n_B and n_C of 1.7 and 1.3 for zinc-doped HBT. Since carbon has significantly lower diffusion coefficient than zinc, it is expected that carbon does not diffuse out through the spacer used in the HBT layer structure. As discussed earlier, this would result in an increase of the base ideality factor [24]. The larger collector current ideality factor observed for carbon-doped HBT is expected to be due to the difference in base-emitter junction between carbon-doped and zinc-doped HBTs; carbon has a lower diffusion coefficient (D_C) than zinc (D_{Zn}) and the base-emitter junction of carbon doped HBTs is consequently expected to be more abrupt than that of zinc-doped HBTs. Since thermionic emission or tunneling of electrons takes place at the more abrupt carbon-doped base-emitter junction, the collector ideality factor of carbon-doped InGaAs base HBTs differs from 1 and is higher than that of zinc-doped InGaAs base HBTs.

IV. Transmission Line Method (TLM) Pattern Analysis for Zinc and Carbon-Doped Base Layers

TLM measurements were performed after base formation and RTA annealing at 375 °C for 7 s. The emitter metal was first evaporated and the layers were then etched down to the base using emitter metal as mask. A selective ethant (HCl/H_3PO_4) was used in order to reach the base.

TLM patterns were fabricated using the same base contact metallization. Typical TLM patterns had a length of 75 μm and width of 150 μm. The TLM gaps ranged from 3 to 50 μm and the base layer was 600 Å thick with a nominal doping concentration for both zinc and carbon-doped base layers of 2×10^{19} cm^{-3}.

The resistance dependence on TLM gap size was evaluated and plotted. It is well known that the total resistance between two TLM contacts with gap L is

$$R_T = 2R_C + R_S \frac{d}{W} \tag{1}$$

where R_C is the contact resistance, R_S is the sheet resistance of base layer, W is the TLM pad width, and d is the TLM gap size. Measurements of zinc and carbon-doped base layers as

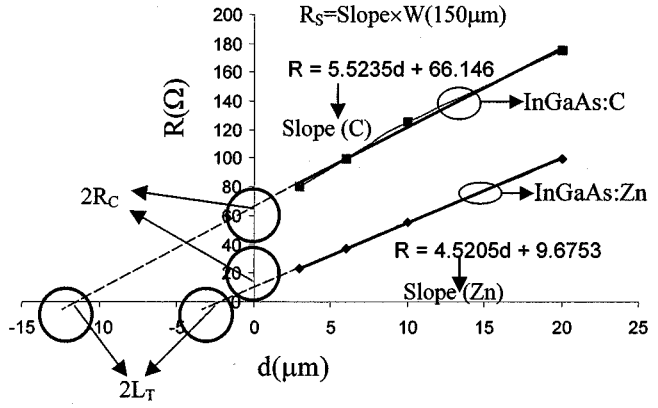

Fig. 3. Plot of total resistance as a function of TLM pad gap size for carbon-doped and zinc-doped InP/InGaAs HBTs.

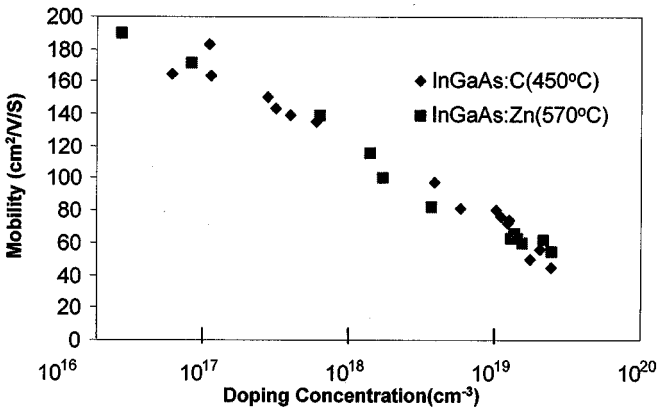

Fig. 4. Hall mobility of carbon-doped InGaAs and zinc-doped InGaAs as a function of doping concentration.

TABLE II
TLM MEASUREMENT RESULTS FOR CARBON-DOPED BASE AND ZINC-DOPED BASE

Study	Base Dopant	Base Dopinng (cm^{-3})	Base Thickness (⇒)	R_s (Ω/⟨)	R_c (Ω)	L_T(μm)
Previous Study [25]	Zn	1.2×10^{19}	600	1433	8.46	0.89
Previous Study [25]	Zn	1.2×10^{19}	600	1349	9.49	1.06
Previous Study [25]	Be	2×10^{19}	2400	210	1.59	1.13
Previous Study [25]	Be	2×10^{19}	3300	148	1.24	1.26
This Study	Zn	2×10^{19}	600	680	4.85	1.06
This Study	C	2×10^{19}	600	828	33.7	5.99

a function of TLM pattern gap size are shown in Fig. 3. The sheet resistance, contact resistance, and transfer length can be calculated from these characteristics.

Typical sheet resistance measurement errors were less than 5%, while the contact resistance and transfer length errors are below 30% and 50%, respectively. The measurement results are summarized in Table II along with several other data obtained for different base doping concentration and base thickness [25].

The sheet resistance of zinc and carbon-doped InGaAs base layers obtained from TLM measurements (680 Ω/□ for zinc and 828 Ω/□ for carbon) is as expected by their nominal doping values (2.0×10^{19} cm^{-3} for both zinc and carbon). The slightly better sheet resistance of zinc-doped (680 Ω/□) than carbon-doped base (828 Ω/□) is due to the slightly higher base doping concentrations of the zinc-doped base. One can estimate the actual base doping concentrations of these two HBTs from their sheet resistance by comparing it with those provided by other studies in Table II. The comparison suggests that the zinc and carbon-doped base concentration is around 2.4×10^{19} cm^{-3} and 2×10^{19} cm^{-3}, respectively.

The sheet resistance of the carbon-doped base (600 Å, 828 Ω/□) is very close to the values reported in [23] (700 Å, 650 Ω/□). It should, however, be noted that in that study [23], a two-step MOCVD growth was employed and postgrowth annealing after base growth was performed with the wafers being placed into the reactor for a second time to regrow the emitter and cap layers. In this study, a simple growth procedure was employed and an optimized InP emitter layer growth was used to restrict the additional hydrogen out-diffusion and improve the base-doping concentration. The employed procedure is much simpler yet led in almost the same value in terms of base sheet resistance.

The contact resistance of the carbon-doped base (33.7 Ω) is found to be much higher than that of zinc-doped base (4.9 Ω) despite their small difference in terms of sheet resistance. The transfer length of the carbon-doped base (5.99 μm) was also larger than that of the zinc-doped base (1.06 μm). The much higher contact resistance and transfer length of the carbon rather than zinc-doped base is not related to doping concentration difference. As mentioned above, the sheet resistance values of these two layers are very similar considering the errors involved in doping calibration. Moreover, the under or over-etching of the base layers should not be the reason either since a selective etchant (HCl/H_3PO_4) with very high selective ratio for InP/InGaAs was used to reach the base.

It should also be pointed out that the difference in terms of contact resistance for zinc and carbon-doped base does not originate from the Hall mobility difference of two layers. Fig. 4 shows the Hall mobility measurement results for zinc and carbon-doped layers over a wide range of doping concentration values. As can be seen, the Hall mobility is not significantly different. For example, for carbon-doped InGaAs layer at a doping concentration of 2.2×10^{19} cm^{-3}, the mobility is about 45 cm^2/V/s whereas for zinc-doped InGaAs layer at a doping concentration of 2.2×10^{19} cm^{-3}, the mobility is about 55 cm^2/V/s. The contact resistance difference caused by mobility variations between zinc and carbon-doped base layers should consequently be marginal.

A possible reason for the observed characteristics is the difference in base-spacer profiles between zinc and carbon doped HBTs. While zinc diffusion causes the 100 Å thick spacer in the zinc-doped HBT to become moderately doped, the 100 Å spacer in carbon doped HBT remains undoped due to the much smaller diffusivity of carbon than that of zinc. As a result, the contact resistance of carbon doped base layer was affected by the thin undoped InGaAs layer under the ohmic contacts.

Annealing after emitter mesa formation, namely, annealing of the HBT layers (500 °C in N_2 for 5 min) after emitter mesas are formed could effectively improve the base sheet resistance [26]. However, as mentioned in [26], it is only effective for HBTs with very narrow emitter widths (< 2 μm). Moreover, this approach is not desirable in our technology since it could severely degrade the InP emitter side-walls and also the exposed base area. Other undesirable effects for emitter ohmic contacts could also be present under such high temperature treatments.

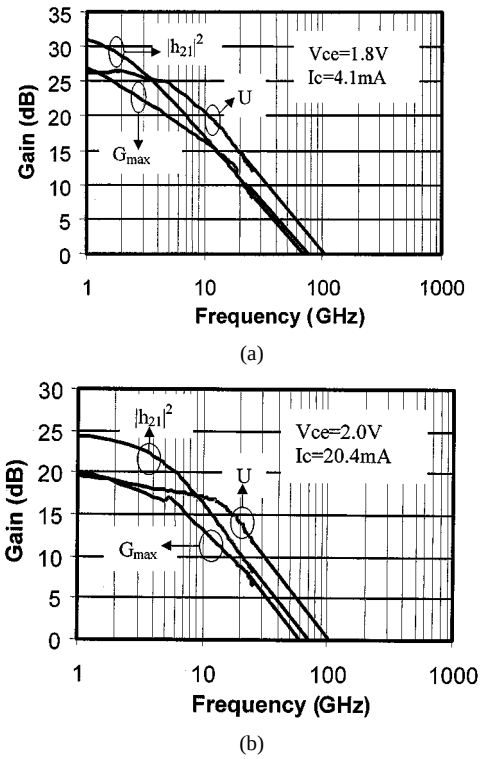

Fig. 5. (a) High-frequency performance of a 1×10 μm^2 zinc-doped InP/InGaAs HBT at $V_{ce} = 1.8$ V and $I_c = 4.1$ mA and (b) high-frequency performance of a 1×10 μm^2 carbon-doped InP/InGaAs HBT at $V_{ce} = 2.0$ V and $I_c = 20.4$ mA.

The HBTs employed in this work typically have a lateral base width of 2 μm self-aligned along the base. For zinc-doped HBTs, the length of lateral contact is almost two times the transfer length (1.06 μm) and appears therefore almost as a semi-infinite contact. On the contrary, for carbon-doped HBTs, the length of the lateral contact is only one third of the transfer length (5.99 μm) and as a result the overall base contact resistance increases in a pronounced way.

The much larger contact resistance of the carbon-doped base layer also causes the increase of the base-emitter voltage of carbon-doped HBTs compared with that of zinc-doped HBTs, as necessary for obtaining the same current density level. For example, at emitter current of 8.7 mA, zinc-doped HBTs have a base-emitter voltage of 0.88 V at $V_{ce} = 1.8$ V while carbon-doped HBTs have a base-emitter voltage of 1.27 V at $V_{ce} = 1.8$ V, almost 0.4 V higher than that of zinc-doped HBT. This is related to the fact that a larger base contact resistance leads to a need for application of higher extrinsic base-emitter voltage in order to achieve the same level of emitter current density.

V. Small-Signal Microwave Performance of Zinc and Carbon-Doped InP/InGaAs HBTs

The small signal S-parameters of zinc and carbon-doped HBTs were measured by using an HP8510B network analyzer from 0.5 GHz to 25.5 GHz. The current gain $|h_{21}|^2$, maximum power gain $G_{\max}$ and unilateral power gain (Mason's gain) were calculated from the measured S-parameters. The cut-off frequency f_T and the maximum frequency of oscillation $f_{\max}$ can be extrapolated by extending the current gain and Mason's gain curve at -20 dB/decade.

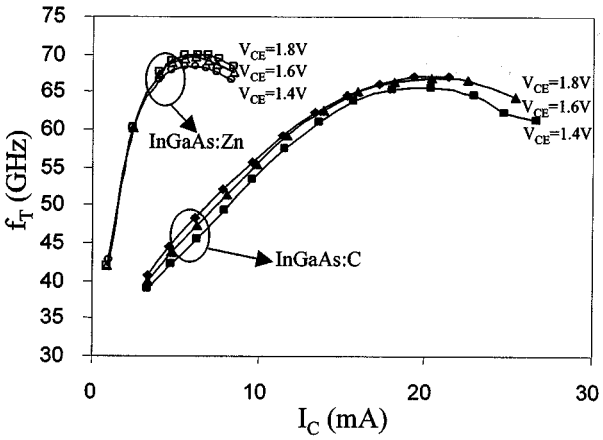

Fig. 6. Dependence of f_T on dc bias for 1×10 μm^2 carbon-doped and zinc-doped InP/InGaAs HBTs.

Fig. 5(a) shows that the bias used for optimal microwave performance of zinc-doped HBTs was $V_{CE} = 1.8$ V, $I_C = 4.1$ mA, corresponding to a current density of 4×10^4 A/cm^2. As can be seen, f_T and $f_{\max}$ of 72 GHz and 109 GHz were achieved under this optimum biasing condition for 1×10 μm^2 zinc-doped HBTs.

Fig. 5(b) shows the high-frequency performance of 1×10 μm^2 carbon-doped HBTs. It is noted that the optimum biasing current ($I_C = 20.4$ mA) is considerably higher than that of 1×10 μm^2 zinc-doped HBTs while V_{CE} was about the same (2.0 V). By using the same extrapolation method as mentioned earlier, f_T and $f_{\max}$ were found to be 70 GHz and 102 GHz, respectively.

In order to explain the large difference between zinc and carbon-doped HBTs in terms of optimum biasing conditions, the microwave performance of these HBTs under different biasing conditions was measured. The dependence of f_T on collector biasing current (I_C) and collector-emitter voltage (V_{CE}) for 1×10 μm^2 zinc and carbon-doped HBTs was plotted in Fig. 6.

The total emitter-to-collector delay τ_{ec} is

$$\begin{aligned}\tau_{ec} =& \frac{1}{2\pi f_T} = \tau_e + \tau_b + \tau_{pcd} + \tau_c = \frac{kT}{qI_E} C_{BE} \\ &+ \left(\frac{W_B^2}{2D_p} + \frac{W_B}{2v_{bc}}\right) + \frac{W_c}{2v_c} + \left(R_c + R_E + \frac{kT}{qI_E}\right) C_{BC} \\ =& \frac{1}{I_E}\left(\frac{kT}{q} C_{BE} + \frac{kT}{q} C_{BC}\right) \\ &+ \left[\left(\frac{W_B^2}{2D_p} + \frac{W_B}{2v_{bc}}\right) + \frac{W_c}{2v_c} + (R_c + R_E) C_{BC}\right] \quad (2)\end{aligned}$$

where τ_e, τ_b, τ_{pcd}, and τ_c are the emitter charging, base transit, precollector delay (time for the electrons to traverse the base-collector depletion region), and collector charging times; W_B is the neutral base width; W_C is the collector depletion width; v_{bc} is the velocity with which electrons are swept into the base collector depletion region; and v_c is the average electron velocity in the collector.

Fig. 7(a) and 7(b) show the plot of τ_{ec} as a function of $1/I_E$ for 1×10 μm^2 zinc and carbon-doped HBTs. One can see that τ_{ec} follows a linear relationship with $1/I_E$ at low current levels. At high current levels, due to the Kirk effects, the effective W_B and C_{BC} increase and therefore, τ_{ec} increases.

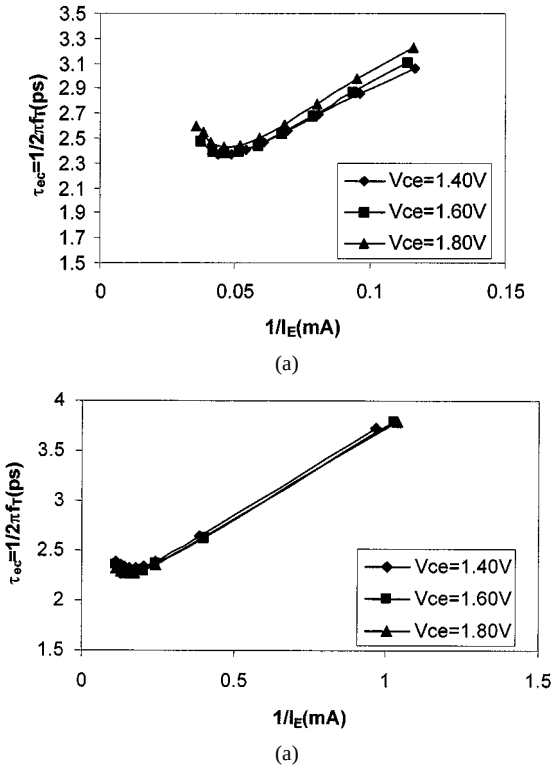

Fig. 7. (a) Plot of τ_{ec} versus $1/I_E$ for $1 \times 10\ \mu\text{m}^2$ carbon-doped InP/InGaAs HBTs and (b) plot of τ_{ec} versus $1/I_E$ for $1 \times 10\ \mu\text{m}^2$ zinc-doped InP/InGaAs HBTs.

By extrapolating the slope and interception of the region where τ_{ec} follows the linear relationship with $1/I_E$ for zinc and carbon-doped HBTs, the slope (Q_d) and the interception (τ') of the curve can be expressed as

$$Q_d = \frac{kT}{q} C_{BE} + \frac{kT}{q} C_{BC} \tag{3}$$

$$\tau' = \left(\frac{W_B^2}{2D_p} + \frac{W_B}{v_{bc}} \right) + \frac{W_c}{2v_c} + (R_c + R_E) C_{BC}. \tag{4}$$

By extending the linear region to $1/I_E = 0$, τ' can be found to be 1.8 ps and 1.9 ps for zinc and carbon-doped HBTs, respectively. This similar performance in terms of τ_{ec} is expected since the base width and collector doping concentration are all the same for these two types of HBTs. As can be seen from (3) and (4), R_C and R_E are also the same due to the same collector/emitter design and growth procedure. The fact that τ' is approximately the same for these two HBTs indicates according to (3) and (4) that the C_{BC} values are similar for these two HBTs. Such similarity is also expected since both collectors are approximately depleted under the collector-emitter bias applied for this study and the collector doping concentration is the same for two HBTs.

However, the slope of the linear region (Q_d) of the τ_{ec} versus I_C dependence shows a large difference between zinc and carbon-doped HBTs. From (3), the sum of C_{BE} and C_{BC} can be evaluated from the slope of the plot as shown in Fig. 7(a) and 7(b) and is found to be 0.07 pF and 0.4 pF for zinc and carbon-doped HBTs, respectively.

C_{BC} values are approximately the same for zinc-doped and carbon-doped HBTs as mentioned above because the base-collector junctions are fully depleted under the applied reverse base-collector bias and the collector designs are the same in terms of doping concentration and thickness. Therefore, the fact that the sum of C_{BE} and C_{BC} for carbon-doped HBTs is much larger than that of zinc-doped HBTs indicates that the base-emitter capacitance of carbon-doped HBTs should be considerably larger than that of zinc-doped devices. As a result, the difference in terms of bias-dependent microwave performance for zinc and carbon-doped HBTs should be mainly due to the considerably larger base-emitter capacitance of carbon-doped HBTs.

The previous results are reasonable considering the Gummel plots of zinc and carbon-doped HBTs shown in Fig. 2(a) and 2(b). The extrinsic base-emitter junction voltage of carbon-doped HBTs is significantly higher than that of zinc-doped HBTs under the same emitter current density. This is partly due to the larger base resistance of carbon-doped HBT, which leads to a more pronounced extrinsic voltage drop across the base resistance, the intrinsic base-emitter junction is, however, not affected directly by this drop. On the other hand, a larger ideality factor for carbon-than zinc-doped HBT (collector current ideality factor n_C of 1.3 and 1.6 for zinc and carbon-doped HBTs, respectively) is observed in Fig. 2(a) and 2(b) due to the difference in base-emitter junctions. This is caused by the lower diffusion coefficient of carbon (D_C) than that of zinc (D_{Zn}) and hence, the base-emitter junction of carbon-doped HBT is expected to be more abrupt than that of zinc-doped HBT. Considering the fact that the built-in voltage of an abrupt n-p heterojunction is $(E_g + \Delta E_c - \Phi_p - \Phi_n)/q$, while that of a graded heteojunction is $(E_g - \Phi_p - \Phi_n)/q$ (Φ_p and Φ_n are the built-in potentials at the p and n-side respectively, E_g is the energy gap on the p-side and ΔE_c is the E-B conduction band discontinuity), one expects that the intrinsic base-emitter junction voltage of carbon-doped HBT is higher than that of zinc-doped HBT at the same current density. The base-emitter junction capacitance of the carbon-doped HBT is therefore larger than that of zinc-doped HBT and contributes to the lower f_T performance of carbon-doped HBT compared with that of zinc-doped HBT at the same current density and also their significant difference in terms of optimum biasing current density for peak f_T performance. (4×10^4 A/cm^2 for zinc HBT and 2×10^5 A/cm^2 for carbon HBT according to the results of Fig. 6).

It is also observed that the maximum frequency of oscillation $f_{\max}(U)$ is similar for zinc and carbon doped HBTs. (109 GHz for zinc-doped and 102GHz for carbon doped HBT). To understand these characteristics, let us first consider $f_{\max}$ and f_T that are related through the following equation (5):

$$f_{\max} = \sqrt{\frac{f_T}{8\pi R_b C_{bc}}}. \tag{5}$$

As discussed previously, carbon-doped HBT has larger base contact resistance while both HBTs have similar f_T (72 GHz for zinc-doped and 70 GHz for carbon doped HBT) and C_{bc}. However, the corresponding current density of carbon-doped HBT (2×10^5 A/cm^2) is much larger than that of zinc-doped HBT (4×10^4 A/cm^2). We therefore attribute the similar $f_{\max}$ performance of carbon-doped HBT and zinc-doped HBT to the base resistance reduction occurring at higher operation current density.

As mentioned earlier, the main difference between the compared HBTs is the base growth procedure and type of base dopant. For zinc-doped HBTs, the entire growth procedure was carried out at the same growth temperature and no growth interruption was introduced except for gas switching. On the other hand, for carbon-doped HBTs, the growth was interrupted before and after the base growth to lower the growth temperature to maximize the p-type doping concentration of the carbon-doped InGaAs base layer. It is shown from the earlier discussion that C_{BE} of carbon-doped HBTs is much larger than that of zinc-doped HBTs under optimum biasing conditions. The growth interruption does not affect the base-collector junction characteristics significantly because the base-collector junction is a homojunction and reverse bias is employed for normal HBT operation. However, the base-emitter junction is severely degraded by this growth interruption and low growth temperature, low V/III ratio employed for carbon-doped base layer growth. Moreover, the low growth temperature and low V/III ratio, which is used for carbon-doped base growth also introduces considerable difficulty in terms of both doping and composition control. As a result, the base contact resistance for carbon-doped base (33.7 Ω) is much higher than that of zinc-doped base (4.9 Ω), although the sheet resistance for these two layers is similar (680 $\Omega/\square$ for zinc-doped base and 828 $\Omega/\square$ for carbon-doped base), indicating the successful growth of highly carbon-doped p-type base (2×10^{19} cm^{-3}).

VI. Conclusion

In this paper, carbon-doped InP/InGaAs HBTs were successfully grown and fabricated by MOCVD. f_T and $f_{\max}(U)$ of 70 GHz and 102 GHz were achieved under optimized bias conditions for these HBTs. At the same time, zinc-doped InP/InGaAs HBTs with the same design except for the base growth procedure and base dopants were grown and fabricated for comparison. It is shown that the dc current gain of carbon-doped HBTs is almost three times lower than that of zinc-doped HBTs. This has been proven by carrier lifetime measurements of zinc and carbon-doped InGaAs layers based on time resolved photoluminescence. It is also shown that the base-emitter voltage of carbon-doped HBTs is much higher than that of zinc-doped HBTs at the same emitter current density. TLM analysis of zinc and carbon-doped InGaAs base layers shows similar sheet resistance. The low sheet resistance of carbon-doped base indicates the successful growth of highly carbon-doped, p-type InGaAs base layers (2×10^{19} cm^{-3}). However, the contact resistance of the carbon-doped base is much larger than that of the zinc-doped base. This is due to the low carbon diffusivity, hydrogen passivation of carbon dopants and base surface degradation, which is caused by the growth interruption before and after base growth, as well as the low temperature and low V/III ratio used for the growth of carbon-doped base. Bias-dependent microwave characteristics of zinc and carbon-doped HBTs were measured and analyzed. It is shown that the optimum biasing conditions for the best microwave performance are considerably different for these two types of HBTs although carbon-doped HBTs have similar f_T and $f_{\max}$ ($f_T = 70$ GHz and $f_{\max} = 102$ GHz, $J_C = 2.0 \times 10^5$ A/cm^2) compared with zinc-doped HBTs ($f_T = 72$ GHz and $f_{\max} = 109$ GHz, $J_C = 4.0 \times 10^4$ A/cm^2) under optimum bias. The analysis shows that the base-emitter junction capacitance of carbon-doped HBTs is much larger than that of zinc-doped HBTs. This larger base-emitter junction capacitance of carbon-doped HBTs is caused by the degraded base-emitter junction, which can be attributed to the low growth temperature, as well as the growth interruption introduced in the procedure of the carbon-doped HBT structure growth.

Acknowledgment

The authors would like to thank Dr. B. Sermage, CNET, France, for the time-resolved photoluminescence characterization of some of the samples.

References

[1] S. Yamahata, K. Krishima, H. Nakajima, T. Kobayashi, and Y. Masuoka, "Ultra-high $f_{\max}$ and f_T InP/InGaAs double-heterojunction bipolar transistors with step-graded InGaAsP collector," in *GaAs IC Symp. Tech. Dig.*, 1994, pp. 345–348.

[2] H.-F. Chau and Y.-C. Kao, "High $f_{\max}$ InAlAs/InGaAs heterojunction bipolar transistors," in *IEDM Tech. Dig.*, 1993, pp. 783–787.

[3] L. Tran, D. Streit, K. Kobayashi, J. Velebir, S. Bui, and A. Oki, "InAlAs/InGaAs HBT with exponentially graded base doping and graded InGaAlAs emitter base junction," in *Proc. 4th Int. Conf. InP and Related Materials*, Newport, RI, 1992, pp. 438–441.

[4] C. Nguyen, T. Liu, M. Chen, H.-C. Sun, and D. Rensch, "AlInAs/GaInAs/InP double heterijunction bipolar transistor with a novel base-collector design for power aplication," *IEEE Electron Device Lett.*, vol. 17, pp. 133–135, Feb. 1996.

[5] J. Cowles, R. Metzger, A. Gutierrez-Aitken, A. Brown, D. Streit, A. Oki, T. Kim, and A. Doolittle, "Double heterojunction bipolar transistors with InP epitaxial layers grown by solid-source MBE," in *Proc. 9th Int. Conf. InP and Related Materials*, Hyannis, MA, 1997, pp. 548–550.

[6] H. Masuda, K. Ouchi, A. Terano, H. Suzuki, K. Watanabe, T. Oka, H. Matsubara, and T. Tanoue, "Device technology of InP/InGaAs HBTs for 40-Gb/s optical transmission application," in *GaAs IC Symp Tech Dig.*, 1997, pp. 139–142.

[7] Y. Matsuoka, H. Nakajima, K. Kurishima, T. Kobayashi, M. Yoneyama, and E. Sano, "Novel InP/InGaAs double-heterojunction bipolar transistors suitable for high-speed ICs and OEICs," in *Proc. 6th Int Conf. On InP and Related Materials*, 1994, pp. 555–558.

[8] P. Enquist, J. A. Hutchby, and T. J. D. Lyon, "Growth and diffusion of abrupt zinc profiles in gallium arseide and heterojunction bipolar transistor structures grown by organometallic vapor phase epitaxy," *J. Appl. Phys.*, vol. 63, pp. 4485–4493, 1988.

[9] K. Hurishma, T. Kobayashi, and U. Gosele, "Abnormal redistribution of Zn in InP/ InGaAs heterojunction bipolar transistor structures," *Appl. Phys. Lett.*, vol. 60, pp. 2496–3498, 1992.

[10] O. Nakajima, H. Ito, T. Nittomo, and K. Nagata, "Current induced degradation of Be-doped AlGaAs/GaAs HBTs and its suppression by Zn diffusion into extrinsic base layer," in *IEDM Tech. Dig.*, San Francisco, CA, 1990.

[11] H. Kong, "Growth of InP-based materials and heterostructures using metalorganic vapor phase epitaxy for high frequency device applications," Ph.D. dissertation, Univ. Michigan, Ann Arbor, 1996.

[12] C. Caneau, R. Bhat, S. Goswami, and M. A. Koza, "OMVPE grown GaInAs:C for HBTs," *J. Electron. Mater.*, vol. 25, pp. 491–495, Mar. 1996.

[13] H. Ito and T. Ishibashi, "Carbon incorporation in (AlGa)As, (AlIn)As and (GaIn)As ternary alloys grown by molecular beam epitaxy," *Jpn. J. Appl. Phys.*, vol. 30, pp. L944–947, 1991.

[14] C. R. Abernathy, S. J. Pearton, F. Ren, W. S. Hobson, and T. R. Fullowan, "Carbon doping of III-V compounds grown by MOMBE," *J. Cryst. Growth*, vol. 105, pp. 375–382, 1990.

[15] T. P. Chin, P. D. Kirchner, J. M. Woodal, and C. W. Tu, "Heavily carbon-doped p-type InGaAs and InGaP by carbon tetracholoride in gas-source molecular beam epitaxy," *Appl. Phys. Lett.*, vol. 59, pp. 2865–2867, 1991.

[16] K. Zhang, W. Hwang, D. L. Miller, and L. W. kapitan, "Carbon doping of InGaAs in solid source molecular beam epitaxy using carbon tetrabromide," *Appl. Phys. Lett.*, vol. 63, pp. 2399–2401, 1994.

[17] C. J. Palmstrom, B. P. Van der Gaag, J.-I. Song, W.-P. Hong, S. A. Swarz, and S. Novak, "Growth of heavy carbon-doped GaInAs lattice matched to InP by chemical beam epitaxy," *Appl. Phys. Lett.*, vol. 64, pp. 3139–3141, 1994.

[18] J.-I. Song, "Chemical beam epitaxy grown carbon-doped base InP/InGaAs heterojunction bipolar transistor technology for millimeter-wave applications," *IEICE Trans. Electron.*, vol. E83-C, pp. 115–121, Jan. 2000.

[19] C. Cheli, D. Cui, S. M. Hubbard, A. Eisenbach, D. Pavlidis, S. K. Krawczyk, and B. Sermage, "Minority carrier lifetime in MOCVD-grown C- and Zn-doped InGaAs," in *Proc. 11th IPRM*, 1999, pp. 127–130.
[20] D. Keiper, B. Sermage, and J.-L. Benchimol, "Influence of zinc co-doping on carbon doped InGaAs," *Jpn. J. Appl. Phys.*, pt. 2, vol. 40, no. 2B, pp. L137–L139, 2001.
[21] S. A. Stockman, A. W. Hanson, S. L. Jackson, J. E. Baker, and G. E. Stillman, "Effect of post-growth cooling ambient on acceptor passivation in cabon-doped GaAs grown by metalorganic chemical vapor deposition," *Appl. Phys. Lett.*, pp. 1248–1250, 1993.
[22] S. A. Stockman, A. W. Hanson, C. M. Colomb, M. T. Fresina, J. E. Baker, and G. E. Stillman, "A comparison of TMGa and TEGa for low temperature metalorganic chemical vapor deposition growth of CCl4-doped InGaAs," *J. Electron. Mat.*, pp. 791–799, 1993.
[23] H. Ito, S. Yamahata, N. Shigekawa, and K. Kurishima, "Heavily carbon-doped base InP/InGaAs heterojunction bipolar transistors grown by two-step metalorganic chemical vapor deposition," *Jpn. J. Appl. Phys.*, vol. 35, pp. 6139–6144, 1996.
[24] B. Hong, J. I. Song, C. Palmstrom, B. Van der Gaag, K. B. Chough, and J. Hayes, "DC, RF and noise characteristics of carbon-doped base InP/InGaAs heterojunction bipolar transistor," *IEEE Trans. Electron Devices*, vol. 41, pp. 19–25, Jan. 1994.
[25] D. Sawdai, "Inp-based NPN and PNP heterojuction bipolar transistor design," in *Technology and Characterization for Enhanced High-Frequency Power Amplification*. Ann Arbor: Univ. Michigan Press, 1999.
[26] K. Kurishima, S. Yamahata, H. Nakajima, H. Ito, and Y. Ishii, "Performance and stability of MOVPE-grown carbon-doped InP/InGaAs HBTs dehydrogenated by an anneal after emitter mesa formation," *Jpn. J. Appl. Phys.*, vol. 37, pp. 1353–1358, 1998.

Delong Cui, photograph and biography not available at the time of publication.

Dimitris Pavlidis (S'73–M'76–SM'83–F'93) received the B.Sc. degree in physics from the University of Patras, Patras, Greece in 1972, and the Ph.D. degree in applied science and electronic engineering from the University of Newcastle, Newcastle-upon-Tyne, U.K., in 1976.

He has been Professor of electrical engineering and computer science at the University of Michigan, Ann Arbor, since 1986. He was an Invited Guest of the Institute of Semiconductor Electronics, Technical University of Aachen, Aachen, Germany, in 1974. He worked as a Postdoctoral Fellow at the University of Newcastle from 1976 to 1978, engaged in work on microwave semiconductor devices and circuits. In 1978, he joined the High Frequency Institute of the Technical University of Darmstadt, Darmstadt, Germany, as a Lecturer working on III-V devices and establishing a new semiconductor technology facility. In 1980, he worked at the Central Electronic Engineering Research Institute, Pilani, India, as a UNESCO Consultant. From 1980 to 1985, he was Engineer and Manager of the GaAs Monolithic Microwave Integrated Circuits (MMIC) Department, Thomson-CSF, Corbeville, France. In this capacity, he was responsible for projects on various monolithic circuits, their technology, and process evaluation. He was a Visiting Scientist with the Centre National d'Études des Télécommunications (CNET)/France Telecom, Bagneux, France, from January to June 1993. Since 1986, he has been involved in research on heterostructure devices and materials at the University of Michigan. This includes the design, fabrication, and characterization of GaAs, InP-based HEMTs and HBTs, diodes for switching and mixing, GaN-based HFETs, and two-terminal devices. His research also covers microwave/ millimeter-wave monolithic heterostructure integrated circuits built with such devices. His materials research covers InP and III-V nitride-based heterostructures using metalorganic chemical vapor deposition (MOCVD) and their device applications. His work in these areas has been reported in numerous papers and reports and he holds six patents.

Prof. Pavlidis was awarded the European Microwave Prize for his work in InP-based monolithic integrated HEMT amplifiers in 1990. In 1991, he received the decoration of "Palmes Académiques" in the Order of Chevalier by the French Ministry of Education for his work in education. In 1992 and 1999, he received the Japan Society of Promotion of Science Fellowship for Senior Scientists/Professors from the Japanese Government and, in 1992, received the Humboldt Research Award for Distinguished Senior U.S. Scientists. He is the recipient of the 1994 University of Michigan Electrical Engineering and Computer Science and the 1996 College of Engineering Research Excellence Awards.

Shawn S. H. Hsu was born in Tainan, Taiwan, R.O.C. He received the B.S. degree from the National Tsing-Hua University, Taiwan, in 1992, the M.S. degree in the Electrical Engineering and Computer Science Department, University of Michigan, Ann Arbor, in 1997, where he is currently pursuing the Ph.D. degree.

From 1992 to 1994, he served as a lieutenant in the military. From 1994 to 1995, he was a Research Assistant with the Institute of Information Management, National Chiao-Tung University, Hsinchu, Taiwan. He joined the III-V Integrated Devices and Circuits Group in 1997. His current research interests include development of analytical and empirical large-signal and noise equivalent circuit models of high-speed III-V/Si-based transistors for RFIC/MMIC design applications, the implementation and development of various measurement techniques to extract parameters for equivalent circuit models, and the design of microwave MMICs and RFIC.

Andreas Eisenbach was born in Romrod, Germany, in 1966. He received the Dipl.-Ing. and Dr.-Ing. degrees in electrical engineering from the Technical University of Darmstadt, Darmstadt, Germany, in 1990 and 1996, respectively, where his research concerned the development of MOVPE growth processes for InP-based OEICs.

From 1996 to 2000, he was a Postdoctoral Research Fellow at the Solid State Electronics Laboratory, University of Michigan, Ann Arbor, where his research area was the MOVPE growth of GaN-based electronic devices as well as InP-based HBTs. In September 2000, he joined IQE, Ltd., Cardiff, U.K., where he is currently involved in the development of MOVPE growth processes for InP- and GaAs-based electronic and optoelectronic devices with emphasis on long-wavelength telecom laser diodes and VCSELs, as well as InP- and GaAs-based HBTs.